

Reply for Reviewer's Comments (Report #1)

Thanks for the positive comments on our submission. We would like to further improve our manuscript following the concrete suggestions.

Line 276: Electrospray ionization does not ionize CHS compounds particularly well, which the authors state. However, CHN compounds are ionized very well in positive mode (while this study only uses negative mode). This should be clarified here. The way it reads now, it sounds like CHN compounds are never ionized well with electrospray, which is not correct.

Line 276-278: We have rephrased the sentence, as follows:

“In general, CHN and CHS compounds are not ionized well in negative ESI mode, which could be a reason why these species were not the most prevalent compounds in this study.”

Line 313: In the discussion of DBEs for CHO and CHON compounds, the authors should note that the double bonds could be present in the O- and/or N- containing functional group OR in the carbon structure. So DBE for CHO or CHON compounds does not necessarily mean that there is a double bond or ring in the carbon structure (it could, but it could also mean

that there is a double bond in the functional group), and thus does not necessarily mean that these compounds show aromaticity. With higher DBE values, actual aromaticity becomes more likely, but at lower DBE values, DBE cannot necessarily be equated to carbon structure double bonds or rings.

Thanks for the constructive comment. We have rephrased the sentence (line 312-317) as follows: “The average double bond equivalent (DBE) showed relatively high values, 5.5 for CHO compounds and 6.1 for CHON compounds (Table S2), suggesting that unsaturated organic compounds were abundant in the present samples, and their presence could partially account for the strong light-absorbing feature in the near-UV region as observed in our previous study (Cai et al., 2018).”

Line 318: Consider reporting average +/- standard deviation as well as the range?

Done. We have rephrased the sentence (line 318-321) as follows:

“Throughout the extract samples, the average H/C and O/C values were ranging from 1.26 ± 0.38 to 1.31 ± 0.40 and from 0.34 ± 0.24 to 0.42 ± 0.29 for CHO compounds, and from 1.19 ± 0.32 to 1.23 ± 0.35 and

from 0.28 ± 0.17 to 0.29 ± 0.15 for CHON compounds (Table S2), respectively.”

Figure 3: It would be helpful to add a few known biomass burning tracers to the figure as anchor points for readers.

Done. We added 4 species to Figure 3 as anchor points, see line 335-339 in the revised text.

Line 418: Are you able to quantify how much water was emitted? Or mention whether there are any literature estimates of this?

Here we do not quantify the content of emitted water. However, previous study have reported that the humidity content in wheat straw was about 13.5% (Bi et al., 2009). Undoubtedly, this substantial water contributed to the formation of burning smog.

line 422-425: We rephrased as follows: “Considering that a substantial amount of water in plant body (Bi et al., 2009) was discharged during the process of straw combustion, the occurrence of phenolic dimers might indicate that the aqueous phase reactions played an important role in the formation and evolution of emitted aerosol organic composition.”

Reference (line 638-639):

Bi, Y., Gao, C., Wang, Y., and Li, B.: Estimation of straw resources in China, Transactions of the Chinese Society of Agricultural Engineering,

Reply for Reviewer's Comments (Report #2)

We would like to thank the reviewer for the constructive comments.

Line 111, change order of techniques, it should be LC coupled with HRMS

Done, see line 111.

Line 276-278. Please clarify the logic of this sentence. The reasoning that something is not easily ionized does imply that there is low abundance of it. On contrary, such species may be underestimated.

Line 276-278: We have rephrased the sentence, as follows:

“In general, CHN and CHS compounds are not ionized well in negative ESI mode, which could be a reason why these species were not the most prevalent compounds in this study.”

Line 279. The word “prefers” is not suitable for this sentence perhaps use “selectively targets”

Done, see line 281.

Line 281, Authors state “there were a number of compounds.” Were these compounds reported in his paper do authors mean “there are” i.e., stating

general fact.

We have revised it.

Line 282, there should be coma after e.g.

Done.

Line 569 insert the space between number and unit.

Done, see line 574 in the revised text.

25 **ABSTRACT**

26 Photochemistry plays an important role in the evolution of atmospheric water soluble
27 organic carbon (WSOC), which dissolves into clouds, fogs and aerosol liquid water. In
28 this study, we tentatively examined the molecular composition and evolution of a
29 WSOC mixture extracted from field-collected wheat straw burning aerosol (WSBA)
30 samples upon photolysis, using direct infusion electrospray ionization (ESI) coupled to
31 high-resolution mass spectrometry (HRMS) and liquid chromatography (LC) coupled
32 with HRMS. For comparison, two typical phenolic compounds (i.e., phenol and
33 guaiacol) emitted from lignin pyrolysis in combination with hydrogen peroxide (H₂O₂)
34 as a typical OH radical precursor were simultaneously exposed to simulated sunlight
35 irradiation. Their photochemical products such as phenolic dimers (e.g., m/z 185.0608
36 for phenol dimer and m/z 245.0823 for guaiacol dimer) or their isomers, were also
37 observed in field-collected WSBA samples, suggesting that the aqueous-phase
38 reactions might contribute to the formation of emitted biomass burning aerosols. The
39 aqueous photochemistry of both the phenols (photooxidation) and WSBA extracts
40 (direct photolysis) could produce a series of highly oxygenated compounds which in
41 turn increases the oxidation degree of organic composition and acidity of the bulk
42 solution. In particular, the LC/ESI-HRMS technique revealed significant
43 photochemical evolution of the WSOC composition in WSBA samples, e.g., the
44 photodegradation of low oxygenated species and the formation of highly oxygenated
45 products. We also tentatively compared the mass spectra of photolytic time-profile
46 WSBA extracts with each other for a more comprehensive description of the photolytic

47 evolution. The calculated average oxygen-to-carbon ratio (O/C) of oxygenated
48 compounds in bulk extract increases from 0.38 ± 0.02 to 0.44 ± 0.02 (mean \pm standard
49 deviation) while the intensity (S/N)-weighted average O/C (O/C_w) increases from 0.45
50 ± 0.03 to 0.53 ± 0.06 as the time of irradiation extends from 0 to 12h. These findings
51 indicate that the water soluble organic fraction of combustion-derived aerosols has the
52 potential to form more oxidized organic matter, contributing to the highly oxygenated
53 nature of atmospheric organic aerosols.

54 **1 INTRODUCTION**

55 Water-soluble organic carbon (WSOC) comprises a significant fraction of
56 atmospheric aerosols, accounting for 20–80% of total organic carbon (OC) (Krivacsy
57 et al., 2001; Wozniak et al., 2008; Fu et al., 2015; Xie et al., 2016). WSOC is directly
58 involved in the formation of cloud condensation nuclei (CCN) by modifying the
59 aqueous chemistry and surface tension of cloud droplets (Graham et al., 2002; Nguyen
60 et al., 2012; Zhao et al., 2013; McNeill 2015). Despite its significance, little is known
61 about the chemical composition and sources of WSOC, with less than 10–20% of the
62 organic mass being structurally identified (Cappiello et al., 2003; Fu et al., 2015).
63 Biomass burning is a well-known emission source of WSOC (Anastasio et al., 1997;
64 Fine et al., 2001; Graham et al., 2002; Mayol-Bracero et al., 2002; Gilardoni et al.,
65 2016). Although the composition varies with fuel type and combustion conditions
66 (Simoneit 2002; Smith et al., 2009), the WSOC mixture often covers a common range
67 of polar and oxygenated aromatic compounds (Graham et al., 2002; Mayol-Bracero et
68 al., 2002; Duarte et al., 2007; Chang and Thompson 2010; Yee et al., 2013; Gilardoni

69 et al., 2016) with molecules incorporating different numbers of functional groups like
70 hydroxyl, carboxyl, aldehyde, ketone, ester, amino and/or other nitrogen-containing
71 groups (Graham et al., 2002). In particular, lignin pyrolysis often yields a large amount
72 of aromatic alcohols, carbonyls, and acid compounds (Mayol-Bracero et al., 2002;
73 Chang and Thompson 2010; Gilardoni et al., 2016). Once dissolved into cloud, fog, and
74 even aerosol liquid water, these substances can undergo aqueous-phase reactions to
75 generate low-volatility species under sunlight irradiation, which have the potential to
76 form secondary organic aerosol (SOA) after water evaporation (Graham et al., 2002;
77 Cappiello et al., 2003; Duarte et al., 2007; Sun et al., 2010; Yu et al., 2014).

78 Field and laboratory studies have demonstrated that aqueous photochemical
79 processes contribute significantly to the aqueous SOA formation from biomass burning
80 precursors and the evolution of smoke particles (Sun et al., 2010; Lee et al., 2011;
81 Kitanovski et al., 2014; Yu et al., 2014; McNeill 2015; Gilardoni et al., 2016). Gilardoni
82 et al. (2016) observed aqueous SOA formation in both fog water and wet aerosols,
83 resulting in an enhancement in the oxidized OA, and following atmospheric aging the
84 overall oxidation degree of aerosols has also increased. In laboratory studies, phenols
85 and methoxyphenols (important biomass burning intermediates) are often used as SOA
86 precursors to examine the photochemical evolution in aqueous environments and
87 aerosol-forming potential under relevant atmospheric conditions (Chang and
88 Thompson 2010; Sun et al., 2010; Smith et al., 2014; Yu et al., 2014; Vione et al., 2019).
89 The corresponding photochemical products formed through hydroxylation,
90 oligomerization, and fragmentation typically cover a series of low-volatility and highly

91 oxygenated species. For instance, the methoxyphenol-derived SOA are proposed as a
92 proxy for atmospheric humic-like substances (HULIS) (Ofner et al., 2011; Yee et al.,
93 2013). Other compounds emitted from lignin pyrolysis, e.g., aromatic alcohol, carbonyl,
94 and carboxylic species retaining the phenyl ring have also been found to produce
95 colored products via aqueous photooxidation, which may become a part of HULIS
96 (Chang and Thompson 2010; Huang et al., 2018). In addition, photochemical
97 processing of common water-soluble aliphatic compounds such as aldehydes (Lim and
98 Turpin 2015), polyols (Daumit et al., 2014), and organic acids (Griffith et al., 2013) in
99 aqueous solution can also lead to the formation of oligomers, highly oxygenated and
100 multifunctional organic matter (McNeill 2015).

101 In recent years, high resolution mass spectrometry (HRMS) has been commonly
102 applied to study the organic molecular composition in cloudwater (Zhao et al., 2013;
103 Boone et al., 2015), fogwater (Cappiello et al., 2003), rainwater (Altieri et al., 2009a;
104 Altieri et al., 2009b), laboratory-generated SOA (Bateman et al., 2011; Romonosky et
105 al., 2015; Lavi et al., 2017), and field-collected aerosol samples (Laskin et al., 2009;
106 Lin et al., 2012a; Lin et al., 2012b; Kourtchev et al., 2013; Tong et al., 2016; Wang et
107 al., 2017). It has also been used in time-profile observations of the photochemical
108 evolution of aqueous extracts from laboratory-generated SOAs (Bateman et al., 2011;
109 Romonosky et al., 2015). However, direct infusion MS methods are prone to ion
110 suppression caused by other organic species, inorganic salts, and adduct formation
111 (Kourtchev et al., 2013). Therefore, liquid chromatography (LC) coupled with HRMS
112 might be another complementary powerful tool for relieving ion suppression due to its

113 abilities to separate and analyze different kind of compounds with differences in LC
114 retention time (Kourtchev et al., 2013; Wang et al., 2016). It could also provide more
115 information enabling the identification of possible isomers from the ions with same
116 mass-to-charge ratio (m/z).

117 To our knowledge, the aqueous photochemical evolution of WSOC extracted from
118 real ambient aerosols has not been studied in detail at the molecular level. Our previous
119 study has revealed that the ultraviolet-visible (UV-VIS) absorption spectra of aqueous
120 extracts from field biomass burning aerosols were modified under simulated sunlight
121 illumination (Cai et al., 2018). Based on the previously studied field-collected samples,
122 the present study is focused on a further analysis to investigate the molecular
123 characteristics of water-soluble organic molecules by the photochemical evolution
124 using electrospray ionization (ESI)-HRMS and LC/ESI-HRMS performed in negative
125 ionization mode. For comparison, we also evaluated the photochemistry of phenol and
126 guaiacol (representing the basic structures of phenols emitted from lignin pyrolysis)
127 under laboratory conditions, and tentatively traced some of their photochemical
128 products (e.g. dimers) in field-collected samples under study.

129 **2 EXPERIMENTAL SECTION**

130 **2.1 Particulate sample collection and preparation of aqueous extracts**

131 The wheat straw burning aerosol (WSBA) samples were collected during the summer
132 harvest season of 2013, at rural fields in the plain of north China where the wheat was
133 the main agricultural crop (Cai et al., 2018). To facilitate subsequent planting and

134 management, a large amount of fresh wheat straw was directly burned in the field during
135 the harvest season, and the water emitted from burning plant body could provide a
136 suitable environment for aqueous photochemistry of dissolved compounds. The
137 selected WSBA samples used for HRMS analysis were collected from two sampling
138 sites, located at rural fields in Wenxian in Henan Province (noted: HNWX) and Daming
139 in Hebei Province (HBDM). As described in Cai et al. (2018), the selected sampling
140 sites were mainly affected by heavy smog from wheat straw burning (Figure 1). The
141 emitted fine particulate matter with aerodynamic diameter $\leq 2.5\mu\text{m}$ ($\text{PM}_{2.5}$) was
142 collected at a flow rate of 5 L min^{-1} by a portable particulate sampler (MiniVol TAS,
143 AirMetrics, USA), with quartz fiber filters (47mm in diameter, QMA, Whatman, UK)
144 baked at 600°C for 6 hours before sampling. The sampling flow rate was calibrated
145 with a standard flow meter (Bios Defender 520) and the sampling time of each filter
146 was restricted to 30-60 minutes depending on the ambient biomass burning aerosol
147 concentration and expected filter loading (Cai et al., 2018). After collection, the filter
148 samples were stored in dark and transported to the laboratory, and then stored at -20°C
149 under a light-proof condition.

150 The preparation of WSOC extracts and measurements for carbon content including
151 organic carbon (OC), elemental carbon (EC) and WSOC were described in detail in Cai
152 et al. (2018). Briefly, a part of each quartz fiber filters ($1.6\text{-}3.2\text{ cm}^2$) was placed into a
153 brown vial and extracted with ultra-pure water (Milli-Q, Milipore) for two times; at
154 each time 5 ml ultra-pure water with a 30 min ultrasonic agitation was applied. The
155 two-time extracts were combined and filtered through a PTFE syringe filter ($0.2\text{ }\mu\text{m}$

156 pore size, Thermo Scientific), followed by a pH measurement with a pH meter (Mettler
157 Toledo SevenEasy™ S20) that has been regularly calibrated at pH 4.00 and 6.86. Prior
158 to analysis the extracts were stored at -20°C in the dark. To reduce the WSOC mass loss,
159 the desalting treatment (e.g., solid phase extraction (SPE)) was not performed on these
160 samples.



161
162 **Figure 1. One field site at Daming, Hebei province, China, for sampling the aerosols affected**
163 **by biomass burning.**

164 **2.2 Direct photolysis of WSOC extracts**

165 A 12-hour direct photolysis of WSOC extracts obtained from WSBA samples was
166 performed in a photo-reactor (BL-GHX-V, Bilon Instruments Co. Ltd., China, see
167 Figure S1) that was equipped with a solar simulator (Xe lamp, 1000W) placed into a
168 double-deck quartz condenser (Cai et al., 2018). A cooling water (18°C) was circulating
169 in the outer tube of the condenser to avoid heating of the samples. In the wavelength
170 range of 310-400 nm relevant to the boundary layer of the atmosphere, the actinic flux

171 of the lamp is about 5 times stronger than the solar actinic flux, meaning that the spectral
172 evolution via the 12-hour simulated solar irradiation might be equal with the effect
173 caused by actual sunlight irradiation with a duration of at least 60 hours (Cai et al.,
174 2018). Air-tight quartz tubes (1.5cm in diameter, 3ml solution per tube) loading extracts
175 were equidistantly arranged around the lamp. Each extract was distributed into three
176 tubes that corresponded to three different irradiation times, i.e. 0, 4, and 12 h, with no
177 oxidants added externally throughout the whole photolytic process. At each irradiation
178 time point (e.g., 0 and 4 h), the related tubes were wrapped with aluminum foil, and
179 placed at the initial location until the end of 12-h photolysis (Cai et al., 2018).

180 As described in Cai et al. (2018), the water extraction resulted in a dilution of the
181 collected organic compounds, however, the ratio of the water mass to PM_{2.5} mass for
182 extract samples (ranging from 1.8×10^3 to 3.4×10^4) was compatible with the ratio of
183 water mass to WSOC content in cloud water (in a wide range from 1.4×10^2 to 1.6×10^4)
184 (Li et al., 2017), indicating that the present aqueous extracts are relevant to the
185 atmospheric cloud water condition.

186 **2.3 Photooxidation of phenolic compounds under laboratory conditions**

187 Initial solutions of 0.1 mM phenol (C₆H₆O) and 0.1 mM guaiacol (C₇H₈O₂) in
188 combination with an OH radical precursor (0.1 mM H₂O₂) were prepared in ultra-pure
189 water (Milli-Q, Milipore). The pH of the solution was adjusted to 5 with 0.1 M sulfuric
190 acid (H₂SO₄), which is usually relevant to the acidity in fog and cloud waters (Collet et
191 al., 1998; Fahey et al., 2005). The prepared solution and reference blank were irradiated
192 by simulated sunlight irradiation with a duration of 4 hours. Hereby, we mainly focus

193 on acquiring the chemical characteristics of aqueous products of phenols, and
194 tentatively identify some tracer compounds (e.g., phenolic dimers) whether they exist
195 in present biomass burning particulate samples.

196 **2.4 Sample analysis**

197 The direct infusion MS analysis was conducted using a Thermo Scientific Orbitrap
198 Fusion Tribrid mass spectrometer equipped with quadrupole, orbitrap, and linear ion
199 trap mass analyzers, with a heated ESI source. To assist in ionization and desolvation,
200 the sample was diluted to a 1:1 mixture of acetonitrile and sample by volume. The full
201 scan mass spectra were acquired in negative ionization mode, with a resolution of
202 120000 at m/z 200 for the Orbitrap analyzer and a mass scan range of m/z 50-750.
203 Before determination, the Orbitrap analyzer was externally calibrated for mass accuracy
204 using Thermo Scientific Pierce LTQ Velos ESI calibration solution. The direct infusion
205 parameters were as follows: sample flow rate $5 \mu\text{l min}^{-1}$; capillary temperature 300°C ;
206 S-lens RF 65%; spray voltage -3.5 kV; sheath gas, auxiliary gas, and sweep gas flows
207 were 10, 3, and 0 arbitrary units, respectively. Data collecting was performed when the
208 intensity of the total ion current (TIC) maintained constant with a relative standard
209 deviation (RSD) under 5%. At least 100 data points (mass spectral scans) were collected
210 for each test sample, and the each exported mass spectrum for analysis was derived
211 from the average result of 100 spectrums.

212 The LC/ESI-HRMS analysis operated in negative ionization mode was performed
213 using a U3000 system coupled with a T3 Atlantis C18 column ($3 \mu\text{m}$; $2.1 \times 150 \text{ mm}$;
214 Waters, Milford, USA) and an Orbitrap Fusion MS. A $10 \mu\text{L}$ sample was injected, with

215 a flow rate of 0.2 ml min⁻¹ for the mobile phase, which consisted of H₂O (A) and
216 acetonitrile (B). The gradient applied was 0-5 min 3% B; 5-20 min from 3 to 95%
217 (linear), and kept for 25 min at 95%; and 45-50 min from 95 to 3%, and held for 10 min
218 at 3% (total run time 60 min).

219 **2.5 Data processing**

220 Mass spectral peaks with three times larger than the signal to noise ratio (S/N) were
221 extracted from the raw files. Peaks in both sample and blank spectra were retained if
222 their intensity in the former was five times larger than in the latter. A common molecular
223 assignment based on the accurate mass was performed using Xcalibur software (V3.0
224 Thermo Scientific) with the following constraints: ¹²C≤50, ¹³C≤1, ¹H≤100, ¹⁶O≤50,
225 ¹⁴N≤4, ³²S≤1, and ³⁴S≤1. All mathematically possible elemental formulas, with a mass
226 tolerance of ±3ppm were calculated. Elemental formulas containing ¹³C or ³⁴S were
227 checked for the presence of ¹²C or ³²S counterparts, respectively. If they were not
228 matched with the corresponding monoisotopic formulas, then the assignment with next
229 larger mass error was considered. Isotopic and unassigned peaks were excluded from
230 further analysis.

231 Ions were also characterized by the number of rings plus double bonds (i.e., double
232 bond equivalents (DBE)), which were calculated as: $DBE = c - h/2 + n/2 + 1$ for an
233 elemental composition of C_cH_hO_oN_nS_s. The assigned formula was additionally checked
234 with the nitrogen rule. For ambient samples, based on the presence of various elements
235 in a molecule, the identified elemental formulas were classified into several main
236 compound classes: CHO (i.e., molecules containing only C, H, and O atoms), CHOS,

237 CHON, and CHONS, and others including CHN and CHS. In the present study, because
238 the detected water-soluble ions almost were below m/z 400, we focused our molecular
239 analysis on m/z 50-400.

240 **3 RESULTS AND DISCUSSION**

241 **3.1 Mass spectral characteristics of WSOC extracts from WSBA samples**

242 The preliminary analysis showed that the $PM_{2.5}$ concentration in ambient air near to
243 the burning sites ranged from 6.46 to 28.03 $mg\ m^{-3}$ (Table S1). OC was the major
244 component of the collected $PM_{2.5}$ with a proportion of $50.9 \pm 7.6\%$ (mean \pm standard
245 deviation), whereas EC represented a negligible fraction (average $1.3 \pm 0.4\%$).
246 Meanwhile, WSOC accounted for $35.5 \pm 7.5\%$ of OC in the tested samples.

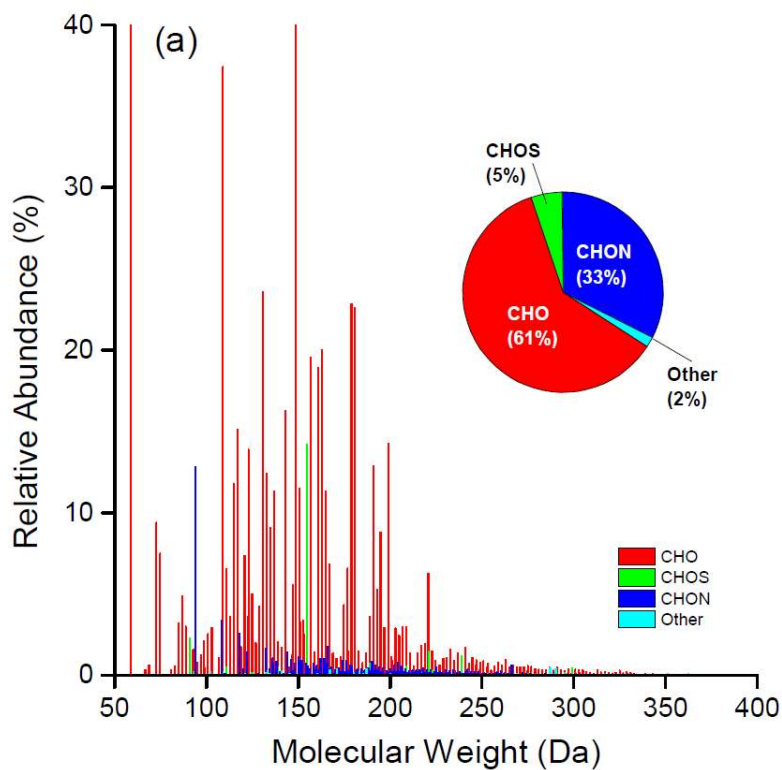
247 Although this batch of aerosol samples were collected from different sites, their
248 water-extracted solutions showed similar light-absorbing characteristics in UV-VIS
249 absorption spectra (Cai et al., 2018). Here, four extract samples (HNWX-1, HNWX-2,
250 HBDM-1 and HBDM-2) (Table S1) were chosen for further analysis using high
251 resolution mass spectrometry. These samples also exhibited similar patterns in mass
252 distribution of water-soluble molecular species that mainly range from 50 to 400 Da,
253 which indicated a similar burning source for these samples. A reconstructed mass
254 spectrum (subtracted blank) for one representative sample of HNWX-1 is shown in
255 Figure 2a (others are shown in Figure S2). In mass range 50-400 Da, there were $827 \pm$
256 44 molecular formulas identified throughout the all samples, and most of the formulas
257 (above 75%) were overlapped between these analyzed samples. The classification
258 features of assigned compounds for analyzed extracts are shown in Table S2. In the

259 amount of assigned formulas, CHO composition was the most abundant group,
260 accounting for $59.2 \pm 2.2\%$ of the total assignments, followed by CHON ($35.0 \pm 2.2\%$).
261 These results are consistent with previous observations of laboratory-generated biomass
262 burning aerosol (Smith et al., 2009) and field particulate samples influenced by biomass
263 combustion (Kourtchev et al., 2016) in spite of the differences of biomass varieties,
264 extracted solvents, and HRMS techniques between present and previous studies.

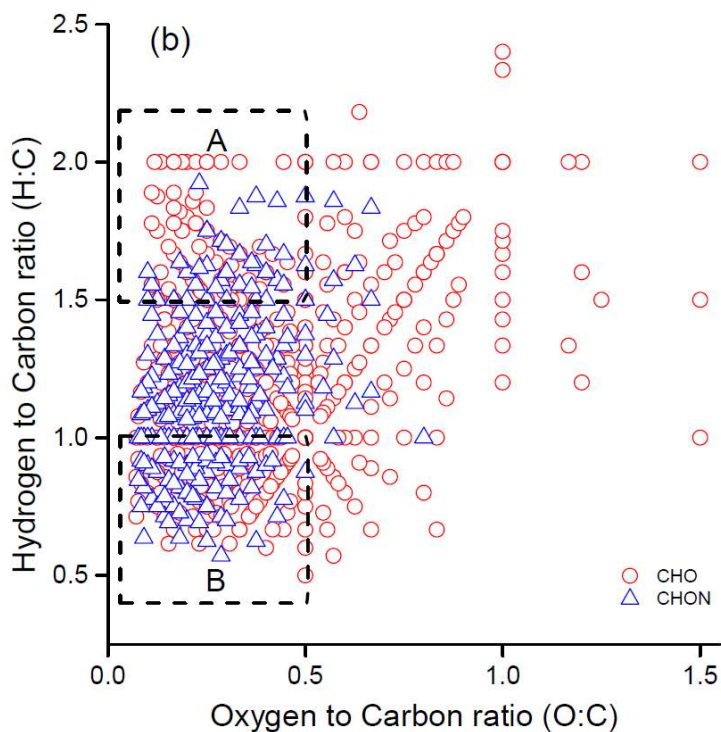
265 On the other hand, CHOS and CHONS compounds contributed with less than 5% to
266 the total assignment. A number of studies have shown the wide presence of
267 organosulfates and nitrooxy-organosulfates in urban (Lin et al., 2012b; Wang et al.,
268 2016), rural (Lin et al., 2012a), and forest aerosols (Kourtchev et al., 2013), and even
269 in cloudwater (Boone et al., 2015); however, most of these compounds were not
270 observed in our negative mass spectra. This could be accounted for by the low extent
271 of aerosol evolution, due to the limited oxidation conditions available for the formation
272 of organosulfates and nitrooxy-organosulfates in fresh smoke aerosols. For example,
273 laboratory studies have observed the significant formation of organosulfates via
274 photooxidation in the presence of acidic sulfate aerosol (with significant level of SO₂
275 concentration) (Surratt et al., 2007; Surratt et al., 2008). All detected ion species with
276 enabled formula assignments in present samples are listed in Table S3. **In general, CHN
277 and CHS compounds are not ionized well in negative ESI mode, which could be a
278 reason why these species were not the most prevalent compounds in this study.**

279 It should be also noted that the negative ionization mode **selectively targets** to detect
280 those molecules containing polar functional groups (e.g., -OH and -COOH) that could

281 be readily deprotonated. There are number of compounds that are not easily
282 deprotonated and might show up preferentially in positive ionization mode (e.g.,
283 amines). Furthermore, the formula numbers detected in the HRMS potentially contain
284 multiple structural isomers; therefore, the actual number of water-soluble organic
285 species is expected to be underestimated. The additional LC/ESI-HRMS analysis
286 operated in negative mode confirmed a substantial number of ion masses (e.g., assigned
287 CHO and CHON compounds) containing more than one structural isomer, which could
288 be observed at different retention times (RTs) in chromatograms. Two representative
289 groups of extracted chromatograms for CHO ($[C_7H_5O_n]^-$, (n=2~4)) and CHON
290 ($[C_7H_5O_nN]^-$, (n=1~3)) compounds are shown in Figure S3 and S4, respectively, where
291 increasing the O or N atom number in a molecule might lead to more isomer peaks.
292 However, it should be noted that these LC-separated peaks might also include other
293 unidentified compounds that were outside of the elemental assignment considered in
294 this study. Additionally, low mass loading and potential decomposition under the
295 ionization can also limit the detection of some high molecular weight species.



296



297

298 **Figure 2. (a) Reconstructed mass spectra for detected ions with assigned formulas and (b)**
 299 **Van Krevelen diagrams for CHO and CHON species in extract of HNWX-1 sample. The**
 300 **inset pie charts in (a) show the number fraction of each class in the total assigned**
 301 **compounds. Areas A and B in (b) are tentatively attributed to aliphatic and aromatic species,**
 302 **respectively.**

303 The interpretation of the complex organic mass spectra generated by high resolution
304 mass spectrometry can be simplified by plotting the hydrogen to carbon ratio (H/C)
305 against the oxygen to carbon ratio (O/C) for individual assigned atomic formulas in
306 form of the Van Krevelen (VK) diagram (e.g. Lin et al., 2012a; Kourtchev et al., 2013).
307 Figure 2b indicates a representative VK diagram of CHO and CHON compounds
308 derived from HNWX-1 sample. It can be clearly seen from Figure 2b that the majority
309 of CHO and CHON molecules are located at the region of $O/C \leq 1.0$ and $H/C \leq 2.0$. In
310 VK diagram, molecules with $H/C \leq 1.0$ and $O/C \leq 0.5$ are typical for aromatic species,
311 while molecules with $H/C \geq 1.5$ and $O/C \leq 0.5$ would be associated with typical
312 aliphatic compounds (Mazzoleni et al., 2012; Kourtchev et al., 2014). The average
313 double bond equivalent (DBE) showed relative high values with 5.5 for CHO
314 compounds and 6.1 for CHON compounds (Table S2), suggesting that unsaturated
315 organic species were abundant in present samples, and their presence could partially
316 account for the strong light-absorbing feature in the near-UV region as observed in our
317 previous study (Cai et al., 2018).

318 Throughout the extract samples, the average H/C and O/C values were ranging from
319 1.26 ± 0.38 to 1.31 ± 0.40 and from 0.34 ± 0.24 to 0.42 ± 0.29 for CHO compounds, and
320 from 1.19 ± 0.32 to 1.23 ± 0.35 and from 0.28 ± 0.17 to 0.29 ± 0.15 for CHON compounds
321 (Table S2), respectively. Although the ESI analysis were performed in the negative
322 ionization mode, the measured O/C exhibit rather low values, which fall in the range of
323 O/C ratios typical for biomass burning organic aerosol derived from positive ionization
324 mode (Aiken et al., 2008; Kourtchev et al., 2016). Due to fresh emission and smaller

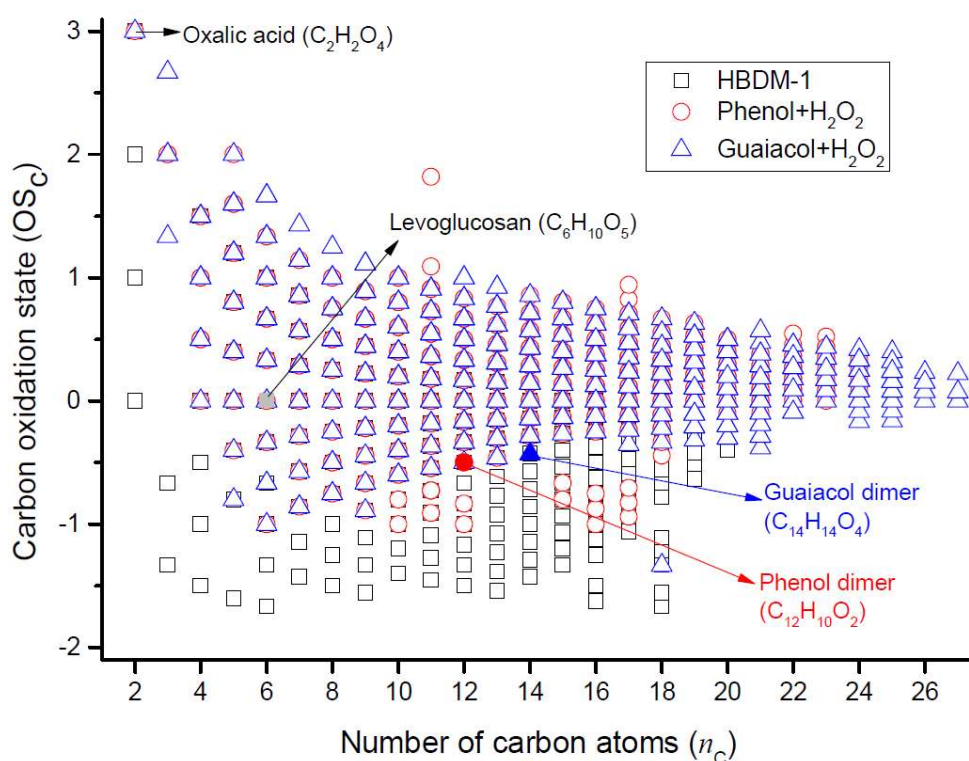
325 aging effect, the present O/C were obviously lower than the O/C of long-range transport
 326 biomass burning aerosols (Zhang et al., 2018).

327 Carbon oxidation state (OS_c) was observed to increase with oxidation for
 328 atmospheric organic aerosol and link strongly to aerosol volatility (Kroll et al., 2011).

329 OS_c for each molecular formula can be calculated using the following equation:

$$330 \quad OS_c = - \sum_i OS_i \frac{n_i}{n_c}$$

331 where OS_i is the oxidation state associated with non-carbon element i and n_i/n_c is the
 332 molar ratio of element i to carbon within the molecule (Kroll et al., 2011; Kourtchev et
 333 al., 2013).



334
 335 **Figure 3. The distribution of carbon oxidation state (OS_c) for CHO molecules in HBDM-1**
 336 **and laboratory samples produced from phenol and guaiacol photooxidation in presence of**
 337 **H_2O_2 (i.e., Phenol+ H_2O_2 and Guaiacol+ H_2O_2). The locations of oxalic acid (identified in**
 338 **HBDM-1 and laboratory samples), levoglucosan (identified in HBDM-1), phenol dimer**
 339 **(identified in Phenol+ H_2O_2), guaiacol dimer (identified in Guaiacol+ H_2O_2) are shown.**

340 Considering that nitrogen and sulfur atoms can present multiple oxidation states, the
341 OSc was calculated and analyzed only for CHO compounds in this study. A similar
342 pattern of OSc values versus the number of carbon atoms (n_C) was observed for CHO
343 compounds detected in present WSBA samples (Figure 3 and Figure S5). From Figure
344 3 and Figure S5, it can be seen that OSc of each sample ranges mainly from -1.5 to +1
345 with average ranging from -0.6 to -0.4. Consistent with previous studies (Kroll et al.,
346 2011; Kourtchev et al., 2016), the majority of molecules with $OS_C < 0$ (low oxidized
347 organics) and carbon atoms lower than 20 are suggested to be associated with the
348 primary organic aerosols emitted from biomass burning. A minor fraction of molecular
349 formulas with $OS_C \geq 0$ values might be associated with semivolatile and low-volatility
350 oxidized organic aerosols (Kroll et al., 2011). Figure 3 also shows the plot of OS_C versus
351 n_C for products obtained from photooxidation of phenol and guaiacol, respectively, and
352 their comparison with WSBA samples will be discussed in section 3.3.

353 **3.2 Mass spectral characteristics of the products from photooxidation of phenolic** 354 **compounds in the aqueous phase**

355 Phenol and guaiacol were chosen as two representative model compounds derived
356 from biomass combustion. Two high resolution mass spectra of aqueous phenol and
357 guaiacol exposed to OH radicals for 4h are shown in Figure S6, where 435 $C_xH_yO_z$
358 molecular formulas (m/z 90-500) were assigned for product ions of phenol (with C_3 -
359 C_{24}) and 624 $C_xH_yO_z$ formulas (m/z 90-600) were assigned for product ions of guaiacol
360 (with C_3 - C_{27}). The average H/C and O/C values were 0.79 ± 0.28 and 0.52 ± 0.23 for
361 phenol, and 0.88 ± 0.24 and 0.59 ± 0.24 for guaiacol, respectively. Clearly, the

362 photochemical processing induced by OH oxidation resulted in an increase in average
363 O/C of product molecules relative to their precursors (O/C = 0.17 for phenol and O/C=
364 0.29 for guaiacol).

365 The formation mechanisms of series of oxygenated products, e.g., phenolic
366 oligomers, hydroxylated phenolic species, ring-opening and highly oxygenated
367 compounds, are proposed in the literature (e.g. Sun et al., 2010; Chang and Thompson,
368 2010; Yu et al., 2014; Huang et al., 2018). The OH-initiated reactions would result in
369 enhanced hydroxylation of the aromatic ring as well as in increased yields of carboxylic
370 acids and toxic dicarbonyl compounds (Sun et al., 2010; Yu et al., 2014; Prasse et al.,
371 2018). For example, some highly oxygenated C₂-C₅ aliphatic compounds (e.g., C₂H₂O₄,
372 C₃H₄O₄, C₄H₆O₄, and C₅H₆O₅) corresponding to carboxylic acids (Yu et al., 2014) were
373 clearly observed in the mass spectra of present photochemical products. The occurrence
374 of these oxygenated products not only directly increased the degree of oxygenation in
375 the bulk solution composition, but also contributed to the variation of solution acidity.
376 After the 4-hours photochemical process, the pH values of the irradiated solution were
377 significantly lower than the pH values of the solution prior to irradiation (t-test, $p < 0.05$),
378 and the calculated acidities ($[H^+]$) of the bulk solution increased by $(2.96 \pm 0.15) \times 10^{-5}$
379 M and $(4.26 \pm 0.16) \times 10^{-5}$ M for phenol and guaiacol, respectively.

380 The oligomerization induced by photochemical transformation of phenolic
381 substances is an important formation pathway for low-volatility, light-absorbing
382 compounds (Smith et al., 2016). Here, phenolic dimers (i.e., C₁₂H₁₀O₂ for phenol
383 dimer and C₁₄H₁₄O₄ for guaiacol dimer) and higher oligomers (e.g., C₁₈H₁₄O₃ and

384 $C_{24}H_{18}O_4$ for phenol trimer and tetramer, $C_{21}H_{20}O_6$ for guaiacol trimer), as well as their
385 hydroxylated species were observed. The formation mechanism can be ascribed to C-
386 O or C-C coupling of phenoxy radicals that were formed via H-abstraction of the
387 phenols or OH addition to the aromatic ring (Net et al., 2009, Sun et al., 2010). The
388 reaction at the para position or para-para coupling was more likely to occur due to a
389 higher probability of free electron to occur in this position (Lavi et al., 2017) or a weaker
390 steric hindrance in the para position.

391 **3.3 Comparison of the photochemical products of phenolic compounds and the** 392 **CHO composition in WSOC extracts from WSBA samples**

393 Compared to the CHO compounds detected in WSOC extracts, the photochemical
394 products of the two phenols under study showed a higher O/C and a lower H/C values.
395 The average OS_C of photochemical products from phenol ($OS_C = -0.7$) and guaiacol
396 ($OS_C = -0.6$) after a 4-hour photooxidation raised to +0.2 and +0.3, respectively,
397 showing distinctly a higher degree of oxidation than the present WSBA samples. In
398 Figure 3, more species with $OS_C < 0$ (especially $OS_C < -0.5$) are presented in the field
399 sample (HBDM-1), while the species with $OS_C \geq 0$ are prevalent in photochemical
400 products of phenol and guaiacol. The single-precursor systems in laboratory did not
401 completely reflect the CHO composition features in water-soluble extracts from real
402 straw-burning samples that contained a myriad of precursors and unknown substances
403 from atmospheric background, soil and other sources. Considering that a large number
404 of phenols and methoxyphenols exist in the straw-burning smokes and their potential
405 to undergo photochemical aging, the nature of emitted primary organic aerosols is

406 reasonably more complicated than the nature of simulated products derived from single-
407 precursor systems.

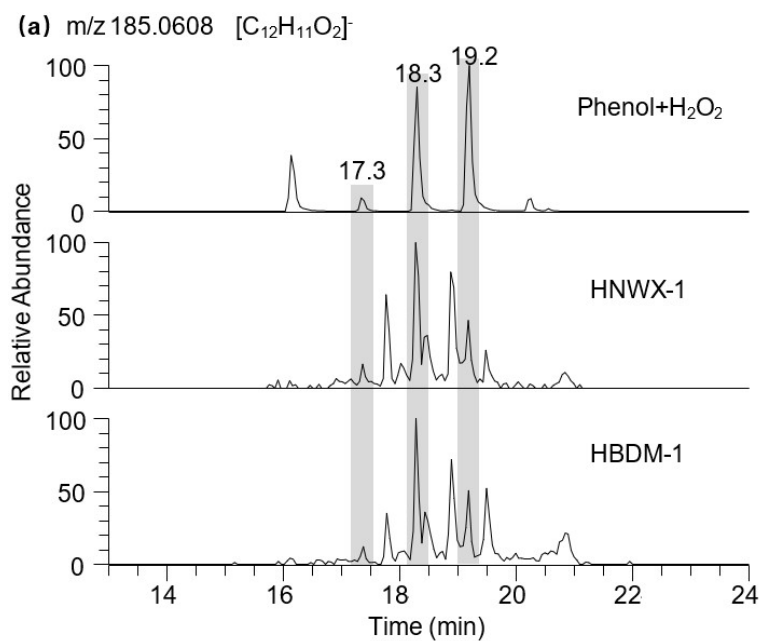
408 The extracted LC chromatograms of m/z 185.0608 and 245.0823 are shown in Figure
409 4, respectively, where both ions involve dimers of phenol and guaiacol with several
410 structures, and/or other isomers. The presence of guaiacol dimer and syringol dimer
411 was previously observed in aerosol samples largely affected by wood combustion.
412 Based on the Aerosol Mass Spectrometer (AMS) analysis, these two dimers were
413 suggested as markers of biomass burning aerosols (Sun et al., 2010; Yu et al., 2014). In
414 the composition of present biomass burning aerosols, the phenolic dimers (m/z
415 185.0608 and 245.0823) were also observed in present mass spectra, but the extracted
416 LC chromatograms shown in Figure 4 indicate that these ions contain multiple RT peaks.
417 The same peaks with RT18.3 and 19.2 min which are assumed to be the phenol dimers
418 were observed during the photochemical transformation of phenol (Figure 4a) and in
419 the WSBA samples. Meanwhile, the present particle extracts may also involve guaiacol
420 dimer, since its m/z 245.0823 has two LC peaks emerged at RT 17.7 and 19.5 min
421 (Figure 4b) same as the peaks identified during the photochemical transformation of
422 guaiacol. Considering that a substantial amount of moisture in plant body (Bi et al.,
423 2009) was discharged during the process of straw combustion, the occurrence of
424 phenolic dimers might indicate that the aqueous phase reactions played an important
425 role in the formation and evolution of emitted aerosol organic composition.

426 Typical hydroxylated species such as, e.g., $C_2H_2O_4$, $C_6H_6O_2$, $C_7H_6O_3$, $C_7H_8O_3$, were
427 also found in the samples from photooxidation of both phenols and the WSBA samples.

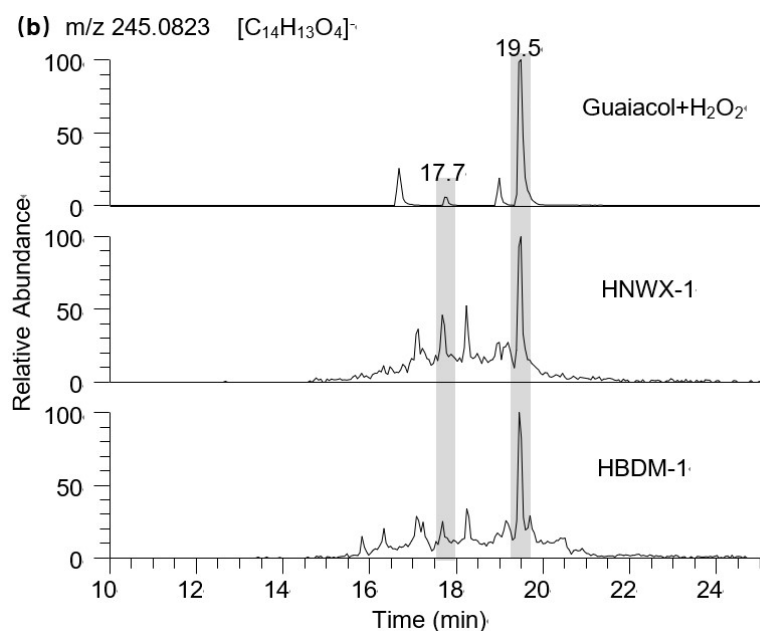
428 The comparison of the photochemical products from phenols and the WSBA samples
429 revealed their significant difference, pointing to the importance of studying real aerosol
430 samples against the laboratory model compounds. However, evaluating the model
431 compounds as proxy of real aerosol samples is always helpful as a reference. To this
432 end, it is worth noting that potentially other phenols and methoxyphenols (e.g.,
433 acetosyringone, vanillin) that dissolve into cloud, fog droplets or aerosol liquid water
434 can be photochemically transformed and contribute to the SOA formation (Vione et al.,
435 2019, Zhou et al., 2019).

436 **3.4 Photolysis of WSOC extracts from WSBA samples**

437 Although the direct photolysis was performed on present WSOC extracts from WSBA
438 samples in presence of simulated sunlight irradiation without adding any oxidants, the
439 photooxidation process still occurred since the particle extracts were very likely to
440 include various oxidants, e.g., singlet molecular oxygen ($^1\text{O}_2$), peroxides, hydroxyl
441 radical (OH) or excited triplet state of organics produced under light excitation
442 (Anastasio et al., 1997; Vione et al., 2006; Net et al., 2009; Net et al., 2010a; Bateman
443 et al., 2011; Rossignol et al., 2014; Smith et al., 2014; Gómez Alvarez et al., 2012). In
444 particular, the excited triplet state of aromatic carbonyls (e.g., 3, 4-
445 dimethoxybenzaldehyde) (Net et al., 2010b) was found to be more efficient than OH
446 radical to oxidize phenols and produce hydroxylated species (Smith et al., 2014., Yu et
447 al., 2014). This photosensitized reaction is likely to play an important role in the WSOC
448 evolution, due to high quantities of aromatic carbonyls present in the extracts of
449 biomass burning aerosols.



450



451

452 **Figure 4. Extracted LC chromatograms of (a) m/z 185.0608 and (b) m/z 245.0823 in**
 453 **photochemical samples of phenols, HNWX-1, and HBDM-1, respectively.**

454 The variation in peak abundance at unique retention times in the chromatogram could
 455 reflect the extent of evolution of WSOC molecules with accurate molecular weights,
 456 although no available standards were utilized for absolute quantification. The LC/ESI-
 457 HRMS monitors obviously changes in the molecular features of partial CHO species,

458 i.e., photodegradation of low oxygenated compounds and formation of high oxygenated
459 compounds. Table 1 lists the CHO compounds for which the LC peak intensities
460 significantly increased and decreased after the 12-hour photolysis.

461 **3.4.1 Photodegradation of low oxygenated compounds and formation of highly** 462 **oxygenated compounds**

463 As shown in Table 1, ion masses assigned with high unsaturated and low oxygenated
464 species ($O/C < 0.5$) are prone to photodegradation, especially C_7 - C_9 compounds
465 (possible aromatic species), which intensity decreased by nearly one order of magnitude.
466 For example, for m/z 123.0450 ($[C_7H_7O_2]^-$), as shown in Figure 5a, the peaks at RT 16.2
467 and 16.7 min in the LC chromatogram reduced in area by 95% after the 12-h irradiation.
468 Using a standard it was verified that both peaks did not belong to guaiacol (peak at
469 RT17.3 min), but they were also found within the products of guaiacol photooxidation,
470 suggesting that they might be isomers of guaiacol or aromatic dihydric alcohol.

471 The phenolic dimers ($C_{12}H_{10}O_2$ and $C_{14}H_{14}O_4$) as described above also exhibited a
472 decreasing tendency with almost complete disappearance after 12h direct photolysis.
473 Other species with relatively high MW (≥ 200 Da) were also observed to be
474 decomposed, including m/z 251.0564 ($[C_{12}H_{11}O_6]^-$), 313.0724 ($[C_{17}H_{13}O_6]^-$), and
475 329.0674 ($[C_{17}H_{13}O_7]^-$) (Figure S7), although their initial abundance was not very high.

476 On the other hand, the solution acidity ($[H^+]$) of the particle extracts increase after
477 the 12-hour photolysis, similar to the observation on the photooxidation of phenols
478 (section 3.2) that resulted in the formation of oxygenated species. The solution acidity
479 ($[H^+]$) normalized by WSOC concentration ($[OC_{ws}]$) was increased with a variation of

480 $\Delta[\text{H}^+]/[\text{OC}_{\text{ws}}] = (3.8 \pm 0.8) \times 10^{-7} \text{ mol mg C}^{-1}$, suggesting the formation of new acidic
 481 substances.

482 **Table 1. *M/Z* with significant changes upon 12-h photolysis analyzed by LC/ESI-HRMS.**

Precursor (LC peak intensity decreases by >50%)			Product (LC peak intensity increases by >50%)		
Retention time, min	Measured <i>m/z</i>	Molecular formula	Retention time, min	Measured <i>m/z</i>	Molecular formula
16.2,16.7	123.04497	C ₇ H ₈ O ₂	1.9	59.01362	C ₂ H ₄ O ₂
13.9,14.5	129.05555	C ₆ H ₁₀ O ₃	1.8	72.99291	C ₂ H ₂ O ₃
14.6	131.07121	C ₆ H ₁₂ O ₃	2.1	73.02928	C ₃ H ₆ O ₂
14.6	133.02934	C ₈ H ₆ O ₂	1.8	75.00856	C ₂ H ₄ O ₃
15.9	135.04498	C ₈ H ₈ O ₂	2.4	85.02930	C ₄ H ₆ O ₂
13.7	137.02426	C ₇ H ₆ O ₃	1.9, 4.4	87.04496	C ₄ H ₈ O ₂
17.7	137.06063	C ₈ H ₁₀ O ₂	1.9	88.98785	C ₂ H ₂ O ₄
15.8	147.04504	C ₉ H ₈ O ₂	1.9	89.02427	C ₃ H ₆ O ₃
17.2	149.06062	C ₉ H ₁₀ O ₂	2.2	99.00857	C ₄ H ₄ O ₃
19.0	151.07634	C ₉ H ₁₂ O ₂	2.5	129.01917	C ₅ H ₆ O ₄
16.8	161.06068	C ₁₀ H ₁₀ O ₂	2.0	145.01407	C ₅ H ₆ O ₅
16.2	165.05559	C ₉ H ₁₀ O ₃	1.9	147.02971	C ₅ H ₈ O ₅
14.9	167.07129	C ₉ H ₁₂ O ₃	14.9	155.03482	C ₇ H ₈ O ₄
15.1	181.05048	C ₉ H ₁₀ O ₄	15.1	169.01411	C ₇ H ₆ O ₅
17.3	191.03498	C ₁₀ H ₈ O ₄	16.4	183.02980	C ₈ H ₈ O ₅
16.2	195.06622	C ₁₀ H ₁₂ O ₄			
18.6	207.06635	C ₁₁ H ₁₂ O ₄			

483 The photochemical processing has led to an increased formation of low MW
 484 compounds (e.g., C₂-C₅ species), with a relatively high O/C. For example, the C₂
 485 compounds, including [C₂H₁O₃]⁻, [C₂H₃O₃]⁻, [C₂H₃O₂]⁻, and [C₂H₁O₄]⁻ (Figure S8),
 486 which may correspond to glyoxylic acid, glycolic acid, acetic acid, and oxalic acid,
 487 respectively, were likely to be formed via oxidation pathway of several water-soluble
 488 molecules with photochemical reactivity (e.g., glyoxal (Carlton et al., 2007; Lim et al.,
 489 2010), methylglyoxal (Altieri et al., 2008; Lim et al., 2010), pyruvic acid (e.g. Grgic et
 490 al., 2010; Griffith et al., 2013; Reed Harris et al., 2014; Rapf et al., 2017; Eugene and

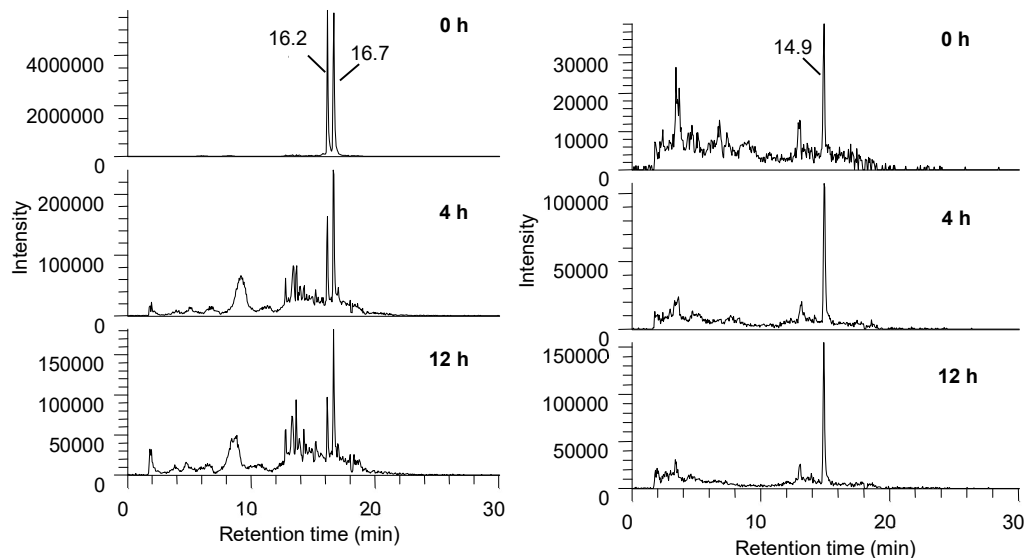
491 Guzman, 2017, Mekic et al., 2018; Mekic et al., 2019), phenols (Sun et al., 2010), etc).
492 The presence of these highly oxygenated compounds that possibly contain acidic
493 groups (e.g., –COOH and –OH) undoubtedly contributed to the increase of the solution
494 acidity. Higher levels of other highly oxygenated species such as $[C_3H_5O_3]^-$, $[C_4H_7O_2]^-$,
495 $[C_5H_5O_5]^-$ and $[C_5H_7O_5]^-$ were also observed (Figure S9).

496 To identify the impact of photolysis on the evolution of specific WSOC, the ions of
497 $[C_7H_7O_n]^-$ in the HBDM-1 sample with significant variation were chosen as
498 representative cases for description. The relative intensity of $[C_7H_7O_2]^-$ and $[C_7H_7O_3]^-$
499 decreased dramatically, while the intensities of $[C_7H_7O_4]^-$, $[C_7H_7O_5]^-$ and $[C_7H_7O_6]^-$
500 increased with the irradiation time (Figure 5 shows only the variation of $[C_7H_7O_2]^-$ and
501 $[C_7H_7O_4]^-$ as an example). It seems reasonable that the possible hydroxylation of
502 $[C_7H_7O_2]^-$ and $[C_7H_7O_3]^-$ might contribute to the formation of $[C_7H_7O_5]^-$ and $[C_7H_7O_6]^-$.
503 Although we could not verify this hypothesis, the formed oxidized species undoubtedly
504 have a high O/C which highlights the possibility of this reaction pathway.

505 **3.4.2 Presentation of photochemically stable organic species**

506 Some of the detected organic species seemed to exhibit a good photochemical
507 stability, as their relative intensities only slightly decreased (<10%) after 12h light
508 irradiation. The m/z 161.0454 ($[C_6H_9O_5]^-$) presented two prominent peaks at RT1.9 and
509 2.4 min (Figure S10). The peak at RT 2.4 min was further confirmed with a standard
510 compound to be levoglucosan, a typical tracer of biomass burning aerosols with a high
511 photochemical stability in atmospheric aerosols (Hu et al., 2013). The relatively good
512 photochemical stability was also observed for some C_6 homolog compounds, such as

513 $[C_6H_7O_6]^-$, $[C_6H_9O_6]^-$, and $[C_6H_{11}O_6]^-$. Some other oxygenated species, such as
514 $[C_3H_3O_3]^-$, $[C_4H_5O_4]^-$, $[C_3H_3O_4]^-$, and $[C_4H_5O_5]^-$ remained relatively stable, as well.



515

516 **Figure 5. Extracted LC chromatograms from HBDM-1 of (a) $[C_7H_7O_2]^-$ and (b) $[C_7H_7O_4]^-$ at**
517 **different photolytic stages of 0, 4, and 12 h.**

518 Regarding the CHON compounds, only small variation of the chromatogram peaks,
519 was observed for most of the detected species. In particular, several species with low
520 O/C decreased by less than 30%, e.g., m/z 94.0297 ($[C_5H_4ON]^-$, RT 7.1 min), and
521 120.0453 ($[C_7H_6ON]^-$, RT12.2 min). Some compounds seem photochemically very
522 stable as the variation of their peak intensities was less than 10 % upon light irradiation
523 of the samples, e.g., m/z 118.0297 ($[C_7H_4ON]^-$, RT16.6 and 17.1 min), 146.0246
524 ($[C_8H_4O_2N]^-$, RT14.4 min), and 190.0510 ($[C_{10}H_8O_3N]^-$, RT17.8 min). However, the
525 intensities of the ion masses with relatively higher degree of oxygenation was found to
526 increase substantially (>50%), e.g., m/z 162.0195 ($[C_8H_4O_3N]^-$, RT 17.2 min), 198.0408
527 ($[C_8H_8O_5N]^-$, RT 18.0 min), and 242.1763 ($[C_{13}H_{24}O_3N]^-$, RT 17.9 min). The
528 photochemical stability of some compounds may be ascribed to their low

529 concentrations, or the light-shielding effect from other light-absorbing species.

530 Another intriguing finding was that different structural isomers with the same
531 molecular mass might have exhibited different fates upon prolonged light irradiation of
532 the samples. For example, the intensity of the peak at m/z 165.0405 ($[C_5H_9O_6]^-$)
533 decreased when it was eluted at 4.9 min, but increased at RT 1.8 min, with the
534 irradiation time (Figure S11). A simultaneous degradation and formation among
535 isomers of some CHON ion masses upon prolonged light irradiation, was also observed,
536 as was the case for the CHO compounds. For example, the m/z 108.0453 assigned to
537 $[C_6H_6ON]^-$, might include hydroxy and amino groups on the phenyl ring to present three
538 possible isomers (Figure S12). During photolytic processing, the intensity of the peak
539 at RT 3.2 min increased dramatically, while there was a clear decreasing tendency of
540 the peak intensity at RT 5.5 and 12.5 min, which was suggestive of possible
541 isomerization among these isomers. Other ion masses that exhibited possible
542 isomerization included m/z 122.0610 ($[C_7H_8ON]^-$), 132.0454 ($[C_8H_6ON]^-$), 134.0245
543 ($[C_7H_4O_2N]^-$), 136.0403 ($[C_7H_6O_2N]^-$), 138.0559 ($[C_7H_8O_2N]^-$), 144.0453 ($[C_9H_6ON]^-$),
544 and 152.0352 ($[C_7H_6O_3N]^-$).

545 **3.4.3 Comparison of time-profile mass spectra of CHO composition in WSOC** 546 **extracts from WSBA samples**

547 Since the LC method just separated a fraction of polar compounds, we tentatively
548 utilized the change of HRMS to gain more comprehensive information about the WSOC
549 evolution. We compared the time-profile (0, 4, and 12h) mass spectra with each other,
550 based on the assumption of same interference from inorganic species, and the good

551 reproducibility and stability for Orbitrap MS operated under the same instrumental
552 parameters (the RSD of TIC intensity within 5%). It is well known that ESI mass
553 spectral abundances are influenced by the solution composition, concentration of
554 analytes and instrumental factors (Bateman et al., 2011); hence, it is quite challenging
555 to directly quantify the absolute concentration levels of the complex mixtures. Despite
556 that, the photochemical degradation of WSOC compounds and corresponding
557 formation of organic compounds can be well described by the variation of signal
558 intensity from mass spectrometry. The average O/C and H/C for CHO compounds were
559 from 0.38 ± 0.02 to 0.44 ± 0.02 and 1.24 ± 0.03 to 1.26 ± 0.01 , respectively, as the
560 irradiation time extended from 0 to 12h. The comparison of these time-profile mass
561 spectra indicates that the 12-hour photolysis resulted in a significant reduction of $28 \pm$
562 11% in the total ion abundance (S/N). Since the photolysis induced changes in
563 abundance for most of the CHO compounds, we also calculated the intensity (S/N)-
564 weighted average O/C (O/C_w) and H/C (H/C_w) (Bateman et al., 2011; Romonosky et
565 al., 2015) with values ranging from 0.45 ± 0.03 to 0.53 ± 0.06 and from 1.32 ± 0.09 to
566 1.40 ± 0.11 , respectively. After the 12-h photolysis, both average H/C and H/C_w values
567 slightly increased, compared to the samples prior to irradiation, however, both average
568 O/C and O/C_w values have increased more distinctly, indicating an elevation in
569 oxidation degree of bulk extract composition. This phenomenon could be partly
570 reflected on the LC-HRMS observation, i.e. formation of highly oxygenated species
571 and the consumption of low oxygenated compounds. In our previous study, the UV-VIS
572 measurements revealed that the 12-h photochemical evolution leads to a modification

573 of absorptive properties for WSBA extracts (e.g., photo-bleaching at wavelengths
574 below 380 nm and photo-enhancement above 380 nm) (Cai et al., 2018), which might
575 be partially linked to present findings about molecular functionalization, e.g.,
576 hydroxylation facilitating a red shift for light absorbing wavelengths.

577 4 CONCLUSIONS

578 This study was focused on the effect of direct photolysis on the molecular
579 composition of actual WSOC extracted from field straw-burning aerosol. The phenol
580 dimer (m/z 185.0608) and guaiacol dimer (m/z 245.0823), or their isomers generated
581 from laboratory aqueous-phase photooxidation of phenol and guaiacol were also
582 observed in present field WSBA samples, suggesting that the aqueous phase reaction
583 might contribute to the formation of emitted biomass burning aerosols. The laboratory
584 observation on aqueous photochemistry of phenols indicated that those phenolic
585 compounds in real biomass burning aerosols would likely have potential to experience
586 similar evolution to form various oxygenated compounds under relevant atmospheric
587 water conditions. The direct photolysis on the molecular composition of WSOC extracts
588 from WSBA samples were performed to gain more insight into the evolution of aerosol
589 composition. Because the extract composition was very complex, the techniques (ESI-
590 HRMS and LC/ESI-HRMS) used in this study, although advanced still had limitations
591 in monitoring the modification of molecular composition, especially for determining
592 the potential formation of compounds present at low concentrations or compounds that
593 were poorly ionized. However, a series of polar molecules were identified that changed
594 their molecular composition via photochemical aging. In particular, the degradation of

595 low oxygenated compounds with strong photochemical reactivity and the formation of
596 high oxygenated compounds might directly result in an increasing O/C in WSOC
597 composition, which was likely linked to the modification of light-absorbing
598 characteristics for extracts in previous study. This finding indicates that the water
599 soluble organic fraction of field combustion-derived aerosols has the potential to form
600 more oxidized organic matter, which might contribute to the highly oxygenated nature
601 of atmospheric organic aerosols. Further studies focused on the photochemical
602 evolution of WSOC composition will be performed in the future, including enlarging
603 measurements on compound species (e.g., applying positive ESI-HRMS), identifying
604 biomarkers and evaluating their role in photochemical processes.

605 **AUTHOR CONTRIBUTION**

606 Jing Cai and Zhiqiang Yu designed the experiments, and Jing Cai and Xiangying Zeng
607 carried them out. Guorui Zhi provided the straw-burning aerosol samples, Zhiqiang Yu
608 and Sasho Gligorovski helped to perform the analysis of light irradiation and editing
609 the manuscript. Guoying Sheng, Xinming Wang and Ping'an Peng provided some
610 technical consultations about organic chemistry. Jing Cai prepared the manuscript with
611 contributions from all co-authors.

612 **ACKNOWLEDGMENTS**

613 This study was financially supported by the National Key Technology Research and
614 Development Program of the Ministry of Science and Technology of China
615 (2014BAC22B04), the National Natural Science Foundations of China (41225013,

616 41530641, 41373131, 41773131, and 41977187) and the Science and Technology
617 Project of Guangdong Province, China (2014B030301060). We are grateful to
618 Guangdong Foundation for Program of Science and Technology Research, Grant N°:
619 2017B030314057.

620 REFERENCES

621 Altieri, K. E., Seitzinger, S. P., Carlton, A. G., Turpin, B. J., Klein, G. C. and Marshall, A. G.: Oligomers
622 formed through in-cloud methylglyoxal reactions: Chemical composition, properties, and
623 mechanisms investigated by ultra-high resolution FT-ICR mass spectrometry. *Atmospheric*
624 *Environment*, 42, 1476-1490, 2008.

625 Altieri, K. E., Turpin, B. J. and Seitzinger, S. P.: Oligomers, organosulfates, and nitrooxy organosulfates
626 in rainwater identified by ultra-high resolution electrospray ionization FT-ICR mass spectrometry,
627 *Atmospheric Chemistry and Physics*, 9, 2533-2542, 2009a.

628 Altieri, K. E., Turpin, B. J. and Seitzinger, S. P.: Composition of Dissolved Organic Nitrogen in
629 Continental Precipitation Investigated by Ultra-High Resolution FT-ICR Mass Spectrometry,
630 *Environmental Science & Technology*, 43, 6950-6955, doi: 10.1021/es9007849, 2009b.

631 Anastasio, C., Faust, B. C. and Rao, C. J.: Aromatic carbonyl compounds as aqueous-phase
632 photochemical sources of hydrogen peroxide in acidic sulfate aerosols, fogs, and clouds .1. Non-
633 phenolic methoxybenzaldehydes and methoxyacetophenones with reductants (phenols),
634 *Environmental Science & Technology*, 31, 218-232, 1997.

635 Bateman, A. P., Nizkorodov, S. A., Laskin, J. and Laskin, A.: Photolytic processing of secondary organic
636 aerosols dissolved in cloud droplets, *Physical Chemistry Chemical Physics*, 13, 12199-12212, doi:
637 10.1039/c1cp20526a, 2011.

638 Bi, Y., Gao, C., Wang, Y., and Li, B.: Estimation of straw resources in China, *Transactions of the Chinese*
639 *Society of Agricultural Engineering*, 25, 211-217, 2009.

640 Boone, E. J., Laskin, A., Laskin, J., Wirth, C., Shepson, P. B., Stirm, B. H. and Pratt, K. A.: Aqueous
641 Processing of Atmospheric Organic Particles in Cloud Water Collected via Aircraft Sampling,
642 *Environmental Science & Technology*, 49, 8523-8530, doi: 10.1021/acs.est.5b01639, 2015.

643 Cai, J., Zhi, G., Yu, Z., Nie, P., Gligorovski, S., Zhang, Y., Zhu, L., Guo, X., Li, P., He, T., He, Y.,
644 Sun, J. and Zhang, Y.: Spectral changes induced by pH variation of aqueous extracts derived from
645 biomass burning aerosols: Under dark and in presence of simulated sunlight irradiation,
646 *Atmospheric Environment*, 185, 1-6, doi: 10.1016/j.atmosenv.2018.04.037, 2018.

647 Cappiello, A., De Simoni, E., Fiorucci, C., Mangani, F., Palma, P., Trufelli, H., Decesari, S., Facchini, M.
648 C. and Fuzzi, S.: Molecular characterization of the water-soluble organic compounds in fogwater
649 by ESIMS/MS, *Environmental Science & Technology*, 37, 1229-1240, doi: 10.1021/es0259990,
650 2003.

651 Chang, J. L. and Thompson, J. E.: Characterization of colored products formed during irradiation of
652 aqueous solutions containing H₂O₂ and phenolic compounds, *Atmospheric Environment*, 44, 541-
653 551, doi: 10.1016/j.atmosenv.2009.10.042, 2010.

654 Carlton, A. G., Turpin, B. J., Altieri, K. E., Seitzinger, S., Reff, A., Lim, H-J. and Ervens, B.: Atmospheric
655 oxalic acid and SOA production from glyoxal: Results of aqueous photooxidation experiments.
656 *Atmospheric Environment*, 41, 7588–7602, 2007.

657 Collett, J.L., Hoag, K.J., Sherman, D.E., Aaron Bator; Richards, W.L. Spatial and temporal variations in
658 San Joaquin Valley fog chemistry, *Atmospheric Environment*, 33 (1), 129-140, 1998. Daumit, K. E.,
659 Carrasquillo, A. J., Hunter, J. F. and Kroll, J. H.: Laboratory studies of the aqueous-phase oxidation
660 of polyols: submicron particles vs. bulk aqueous solution, *Atmospheric Chemistry and Physics*, 14,
661 10773-10784, doi: 10.5194/acp-14-10773-2014, 2014.

662 Duarte, R. M. B. O., Santos, E. B. H., Pio, C. A. and Duarte, A. C.: Comparison of structural features of
663 water-soluble organic matter from atmospheric aerosols with those of aquatic humic substances,
664 *Atmospheric Environment*, 41, 8100-8113, doi: 10.1016/j.atmosenv.2007.06.034, 2007.

665 Eugene, A. J. and Guzman, M. I. Reactivity of Ketyl and Acetyl Radicals from Direct Solar Actinic
666 Photolysis of Aqueous Pyruvic Acid. *Journal of Physical Chemistry A*, 121, 2924–2935, 2017.

667 Fahey, K. M., Pandis, S. N., Collett, J. L. and Herckes, P. The influence of size-dependent droplet
668 composition on pollutant processing by fogs, *Atmospheric Environment*, 39(25), 4561-4574, 2005.

669 Fine, P. M., Cass, G. R. and Simoneit, B. R. T.: Chemical characterization of fine particle emissions from
670 fireplace combustion of woods grown in the northeastern United States, *Environmental Science &*
671 *Technology*, 35, 2665-2675, 2001.

672 Fu, P. Q., Kawamura, K., Chen, J., Qin, M. Y., Ren, L. J., Sun, Y. L., Wang, Z. F., Barrie, L. A., Tachibana,

673 E., Ding, A. J. and Yamashita, Y.: Fluorescent water-soluble organic aerosols in the High Arctic
674 atmosphere, *Scientific Reports*,5, 2015.

675 Gilardoni, S., Massoli, P., Paglione, M., Giulianelli, L., Carbone, C., Rinaldi, M., Decesari, S., Sandrini,
676 S., Costabile, F., Gobbi, G. P., Pietrogrande, M. C., Visentin, M., Scotto, F., Fuzzi, S. and Facchini,
677 M. C.: Direct observation of aqueous secondary organic aerosol from biomass-burning emissions,
678 *Proceedings of the National Academy of Sciences of the United States of America*,113, 10013-
679 10018, 2016.

680 Gómez Alvarez, E., Wortham, H., Strekowski, R., Zetzsch, C., S. Gligorovski,S.: Atmospheric photo-
681 sensitized heterogeneous and multiphase reactions: From outdoors to indoors, *Environmental*
682 *Science & Technology*, 46, 1955-1963, 2012.

683 Graham, B., Mayol-Bracero, O. L., Guyon, P., Roberts, G. C., Decesari, S., Facchini, M. C., Artaxo, P.,
684 Maenhaut, W., Koll, P. and Andreae, M. O.: Water-soluble organic compounds in biomass burning
685 aerosols over Amazonia-1. Characterization by NMR and GC-MS, *Journal of Geophysical*
686 *Research-Atmospheres*,107, doi: 10.1029/2001jd000336, 2002.

687 Grgic, I., Nieto-Gligorovski, L.I., Net, S., Temime-Roussel, B., Gligorovski, S. and Wortham, H.: Light
688 induced multiphase chemistry of gas-phase ozone on aqueous pyruvic and oxalic acids, *Physical*
689 *Chemistry Chemical Physics*, 12, 698-707, 2010.

690 Griffith, E. C., Carpenter, B. K., Shoemaker, R. K. and Vaida, V.: Photochemistry of aqueous pyruvic
691 acid, *Proceedings of the National Academy of Sciences of the United States of America*,110, 11714-
692 11719, doi: 10.1073/pnas.1303206110, 2013.

693 Hu, Q., Xie, Z., Wang, X., Hui Kang, H. and Zhang, P.: Levoglucosan indicates high levels of biomass
694 burning aerosols over oceans from the Arctic to Antarctic, *Scientific Reports*, 3, 2013.

695 Kitanovski, Z., Cusak, A., Grgic, I. and Claeys, M.: Chemical characterization of the main products
696 formed through aqueous-phase photolysis of guaiacol, *Atmospheric Measurement Techniques*,7,
697 2457-2470, doi: 10.5194/amt-7-2457-2014, 2014.

698 Kroll, J. H., Donahue, N. M., Jimenez, J. L., Kessler, S. H., Canagaratna, M. R., Wilson, K. R., Altieri, K.
699 E., Mazzoleni, L. R., Wozniak, A. S., Bluhm, H., Mysak, E. R., Smith, J. D., Kolb, C. E., and Worsnop,
700 D. R.: Carbon oxidation state as a metric for describing the chemistry of atmospheric organic aerosol,
701 *Nat. Chem. Biol.*, 3, 133–139, 2011.

702 Kourtchev, I., Fuller, S., Aalto, J., Ruuskanen, T. M., McLeod, M. W., Maenhaut, W., Jones, R., Kulmala,

703 M. and Kalberer, M.: Molecular Composition of Boreal Forest Aerosol from Hyytiälä, Finland,
704 Using Ultrahigh Resolution Mass Spectrometry, *Environmental Science & Technology*, 47, 4069-
705 4079, doi: 10.1021/es3051636, 2013.

706 Kourtchev, I., Godoi, R. H. M., Connors, S., Levine, J.G., Archibald, A.T., Godoi, A. F. L., Paralovo,
707 S.L., Barbosa, C. G. G., Souza, R. A. F., Manzi, A. O., Seco, R., Sjostedt, S., Park, J. H., Guenther
708 A., Kim, S., Smith, J., Martin, S. T., and Kalberer, M.: Molecular composition of organic aerosols
709 in central Amazonia: an ultra-high-resolution mass spectrometry study, *Atmospheric Chemistry
710 and Physics*, 16, 11899–11913, 2016.

711 Krivacsy, Z., Hoffer, A., Sarvari, Z., Temesi, D., Baltensperger, U., Nyeki, S., Weingartner, E., Kleefeld,
712 S. and Jennings, S. G.: Role of organic and black carbon in the chemical composition of atmospheric
713 aerosol at European background sites, *Atmospheric Environment*, 35, 6231-6244, 2001.

714 Laskin, A., Smith, J. S. and Laskin, J.: Molecular Characterization of Nitrogen-Containing Organic
715 Compounds in Biomass Burning Aerosols Using High-Resolution Mass Spectrometry,
716 *Environmental Science & Technology*, 43, 3764-3771, doi: 10.1021/es803456n, 2009.

717 Lavi, A., Lin, P., Bhaduri, B., Carmieli, R., Laskin, A. and Rudich Y.: Characterization of light-absorbing
718 oligomers from reactions of phenolic compounds and Fe(III), *Earth and Space Chemistry*, 1, 637-646,
719 2017.

720 Lee, A. K. Y., Herckes, P., Leaitch, W. R., Macdonald, A. M. and Abbatt, J. P. D.: Aqueous OH oxidation
721 of ambient organic aerosol and cloud water organics: Formation of highly oxidized products,
722 *Geophysical Research Letters*, 38, 2011.

723 Lim, Y. B., Tan, Y., Perri, M. J., Seitzinger, S. P. and Turpin, B. J.: Aqueous chemistry and its role in
724 secondary organic aerosol (SOA) formation, *Atmospheric Chemistry and Physics*, 10, 10521-10539,
725 doi: 10.5194/acp-10-10521-2010, 2010.

726 Lim, Y. B. and Turpin, B. J.: Laboratory evidence of organic peroxide and peroxyhemiacetal formation
727 in the aqueous phase and implications for aqueous OH, *Atmospheric Chemistry and Physics*, 15,
728 12867-12877, doi: 10.5194/acp-15-12867-2015, 2015.

729 Lin, P., Rincon, A. G., Kalberer, M. and Yu, J. Z.: Elemental Composition of HULIS in the Pearl River
730 Delta Region, China: Results Inferred from Positive and Negative Electrospray High Resolution
731 Mass Spectrometric Data, *Environmental Science & Technology*, 46, 7454-7462, doi:
732 10.1021/es300285d, 2012a.

733 Lin, P., Yu, J. Z., Engling, G. and Kalberer, M.: Organosulfates in Humic-like Substance Fraction Isolated
734 from Aerosols at Seven Locations in East Asia: A Study by Ultra-High-Resolution Mass
735 Spectrometry, *Environmental Science & Technology*, 46, 13118-13127, doi: 10.1021/es303570v,
736 2012b.

737 Mayol-Bracero, O. L., Guyon, P., Graham, B., Roberts, G., Andreae, M. O., Decesari, S., Facchini, M.
738 C., Fuzzi, S. and Artaxo, P.: Water-soluble organic compounds in biomass burning aerosols over
739 Amazonia - 2. Apportionment of the chemical composition and importance of the polyacidic
740 fraction, *Journal of Geophysical Research-Atmospheres*, 107, doi: 10.1029/2001jd000522, 2002.

741 McNeill, V. F.: Aqueous Organic Chemistry in the Atmosphere: Sources and Chemical Processing of
742 Organic Aerosols, *Environmental Science & Technology*, 49, 1237-1244, 2015.

743 Mekic, M., Loisel, G., Zhou, W., Jiang, B., Vione, D., Gligorovski, S.: Ionic strength effects on the reactive
744 uptake of ozone on aqueous pyruvic acid: Implications for air-sea ozone deposition, *Environmental
745 Science and Technology*, 52, 12306–12315, 2018.

746 Mekic, M., Liu, J., Zhou, W., Loisel, G., Cai, J., He, T., Jiang, B., Yu, Z., Lazarou, Y. G., Li, X., Brigante,
747 M., Vione, D., Gligorovski, S.: Formation of highly oxygenated multifunctional compounds from
748 cross-reactions of carbonyl compounds in the atmospheric aqueous phase, *Atmospheric
749 Environment*, 219, 117046, 2019.

750 Net, S., Nieto-Gligorovski, L., Gligorovski, S., Temime-Rousell, B., Barbati, S., Lazarou, Y. G., and
751 Wortham, H.: Heterogeneous light induced ozone processing on the organic coatings in the
752 atmosphere, *Atmospheric Environment*, 43, 1683-1692, 2009.

753 Net, S., Nieto-Gligorovski, L., Gligorovski, S., and Wortham, H.: Heterogeneous ozonation kinetics of 4-
754 phenoxyphenol in presence of photosensitizer, *Atmospheric Chemistry and Physics*, 10, 1545-1554,
755 2010b.

756 Net, S., Gligorovski, S., and Wortham, H.: Light-induced heterogeneous ozone processing on organic
757 coated particles: Kinetics and condensed-phase products, *Atmospheric Environment*, 44, 3286-3294,
758 2010b.

759 Nguyen, T. B., Lee, P. B., Updyke, K. M., Bones, D. L., Laskin, J., Laskin, A. and Nizkorodov, S. A.:
760 Formation of nitrogen- and sulfur-containing light-absorbing compounds accelerated by
761 evaporation of water from secondary organic aerosols, *Journal of Geophysical Research-
762 Atmospheres*, 117, doi: 10.1029/2011jd016944, 2012.

763 Ofner, J., Krueger, H. U., Grothe, H., Schmitt-Kopplin, P., Whitmore, K. and Zetzsch, C.: Physico-
764 chemical characterization of SOA derived from catechol and guaiacol - a model substance for the
765 aromatic fraction of atmospheric HULIS, *Atmospheric Chemistry and Physics*, 11, 1-15, doi:
766 10.5194/acp-11-1-2011, 2011.

767 Petzold, A., Kopp, C., Niessner, R., 1997. The dependence of the specific attenuation cross-section on
768 black carbon mass fraction and particle size. *Atmospheric Environment*, 31, 661-672, 1997.

769 Prasse, C., Ford, B., Nomura, D.K. and Sedlak, D.L.: Unexpected transformation of dissolved phenols
770 to toxic dicarbonyls by hydroxyl radicals and UV light, <https://doi.org/10.1073/pnas.1715821115>,
771 2018.

772 Rapf, R. J., Perkins, R. J., Carpenter, B. K. and Vaida, V.: Mechanistic Description of Photochemical
773 Oligomer Formation from Aqueous Pyruvic Acid. *Journal of Physical Chemistry A*, 121, 4272–4282,
774 2017.

775 Reed Harris, A. E., Ervens, B., Shoemaker, R. K., Kroll, J. A., Rapf, R. J., Griffith, E. C., Monod, A.,
776 Vaida, V.: Photochemical kinetics of pyruvic acid in aqueous solution. *Journal of Physical
777 Chemistry A*, 118 (37), 8505–8516, 2014.

778 Romonosky, D. E., Laskin, A., Laskin, J. and Nizkorodov, S. A.: High-Resolution Mass Spectrometry
779 and Molecular Characterization of Aqueous Photochemistry Products of Common Types of
780 Secondary Organic Aerosols, *Journal of Physical Chemistry A*, 119, 2594-2606, doi:
781 10.1021/jp509476r, 2015.

782 Rossignol, S., Areghegn, K. Z., Tinel, L., Fine, L., Noziere, B. and George, C.: Glyoxal Induced
783 Atmospheric Photosensitized Chemistry Leading to Organic Aerosol Growth, *Environmental
784 Science & Technology*, 48, 3218-3227, 2014.

785 Simoneit, B. R. T.: Biomass burning - A review of organic tracers for smoke from incomplete combustion,
786 *Applied Geochemistry*, 17, 129-162, doi: 10.1016/s0883-2927(01)00061-0, 2002.

787 Smith, J. D., Sio, V., Yu, L., Zhang, Q. and Anastasio, C.: Secondary Organic Aerosol Production from
788 Aqueous Reactions of Atmospheric Phenols with an Organic Triplet Excited State, *Environmental
789 Science & Technology*, 48, 1049-1057, doi: 10.1021/es4045715, 2014.

790 Smith, J. S., Laskin, A. and Laskin, J.: Molecular Characterization of Biomass Burning Aerosols Using
791 High-Resolution Mass Spectrometry, *Analytical Chemistry*, 81, 1512-1521, doi: 10.1021/ac8020664,
792 2009.

793 Smith, J. D., Kinney, H. and Anastasio, C.: Phenolic carbonyls undergo rapid aqueous photodegradation
794 to form low-volatility, light-absorbing products, *Atmospheric environment*, 126, 36-44, 2015.

795 Sun, Y. L., Zhang, Q., Anastasio, C. and Sun, J.: Insights into secondary organic aerosol formed via
796 aqueous-phase reactions of phenolic compounds based on high resolution mass spectrometry,
797 *Atmospheric Chemistry and Physics*, 10, 4809-4822, doi: 10.5194/acp-10-4809-2010, 2010.

798 Surratt, J. D., Gomez-Gonzalez, Y., Chan, A. W. H., Vermeylen, R., Shahgholi, M., Kleindienst, T. E.,
799 Edney, E. O., Offenberg, J. H., Lewandowski, M., Jaoui, M., Maenhaut, W., Claeys, M., Flagan, R.
800 C. and Seinfeld, J. H.: Organosulfate formation in biogenic secondary organic aerosol, *Journal of*
801 *Physical Chemistry A*, 112, 8345-8378, doi: 10.1021/jp802310p, 2008.

802 Surratt, J. D., Kroll, J. H., Kleindienst, T. E., Edney, E. O., Claeys, M., Sorooshian, A., Ng, N. L.,
803 Offenberg, J. H., Lewandowski, M., Jaoui, M., Flagan, R. C. and Seinfeld, J. H.: Evidence for
804 organosulfates in secondary organic aerosol, *Environmental Science & Technology*, 41, 517-527, doi:
805 10.1021/es062081q, 2007.

806 Tong, H., Kourtchev, I., Pant, P., Keyte, I. J., O'Connor, I. P., Wenger, J. C., Pope, F. D., Harrison, R. M.
807 and Kalberer, M.: Molecular composition of organic aerosols at urban background and road tunnel
808 sites using ultra-high resolution mass spectrometry. *Faraday Discussions*, 189, 51-68, 2016.

809 Vione, D., Maurino, V., Minero, C., Pelizzetti, E., Harrison, M. A. J., Olariu, R. I. and Arsene, C.:
810 Photochemical reactions in the tropospheric aqueous phase and on particulate matter, *Chemical*
811 *Society Reviews*, 35, 441-453, 2006.

812 Vione, V., Albinet, A., Barsotti, F., Mekic, M., Jiang, B., Minero, C., Brigante, M., Gligorovski, S.:
813 Formation of substances with humic-like fluorescence properties, upon photoinduced
814 oligomerization of typical phenolic compounds emitted by biomass burning, *Atmospheric*
815 *Environment*, <https://doi.org/10.1016/j.atmosenv.2019.03.005>, 2019.

816 Wang, X. K., Rossignol, S., Ma, Y., Yao, L., Wang, M. Y., Chen, J. M., George, C. and Wang, L.:
817 Molecular characterization of atmospheric particulate organosulfates in three megacities at the
818 middle and lower reaches of the Yangtze River, *Atmospheric Chemistry and Physics*, 16, 2285-2298,
819 2016.

820 Wang, X., Hayeck, N., Brüggemann, M., Yao, L., Chen, H., Zhang, C., Emmelin, C., Jianmin Chen, J.,
821 George, C. and Lin Wang, L. Chemical characteristics of organic aerosols in shanghai: A study by
822 ultrahigh-performance liquid chromatography coupled with Orbitrap mass spectrometry, *Journal of*

823 Geophysical Research-Atmospheres, 122 (11), 703–722, 2017.

824 Wozniak, A. S., Bauer, J. E., Sleighter, R. L., Dickhut, R. M. and Hatcher, P. G.: Technical Note:
825 Molecular characterization of aerosol-derived water soluble organic carbon using ultrahigh
826 resolution electrospray ionization Fourier transform ion cyclotron resonance mass spectrometry,
827 Atmospheric Chemistry and Physics, 8, 5099-5111, 2008.

828 Xie, M. J., Mladenov, N., Williams, M. W., Neff, J. C., Wasswa, J. and Hannigan, M. P.: Water soluble
829 organic aerosols in the Colorado Rocky Mountains, USA: composition, sources and optical
830 properties, Scientific Reports, 6, 2016.

831 Yee, L. D., Kautzman, K. E., Loza, C. L., Schilling, K. A., Coggon, M. M., Chhabra, P. S., Chan, M. N.,
832 Chan, A. W. H., Hersey, S. P., Crounse, J. D., Wennberg, P. O., Flagan, R. C. and Seinfeld, J. H.:
833 Secondary organic aerosol formation from biomass burning intermediates: phenol and
834 methoxyphenols, Atmospheric Chemistry and Physics, 13, 8019-8043, 2013.

835 Yu, L., Smith, J., Laskin, A., Anastasio, C., Laskin, J. and Zhang, Q.: Chemical characterization of SOA
836 formed from aqueous-phase reactions of phenols with the triplet excited state of carbonyl and
837 hydroxyl radical, Atmospheric Chemistry and Physics, 14, 13801-13816, doi: 10.5194/acp-14-
838 13801-2014, 2014.

839 Zhao, Y., Hallar, A. G. and Mazzoleni, L. R.: Atmospheric organic matter in clouds: exact masses and
840 molecular formula identification using ultrahigh-resolution FT-ICR mass spectrometry,
841 Atmospheric Chemistry and Physics, 13, 12343-12362, doi: 10.5194/acp-13-12343-2013, 2013.

842 Zhi, G., Chen, Y., Xue, Z., Meng, F., Cai, J., Sheng, G. and Fu, J.: Comparison of elemental and black
843 carbon measurements during normal and heavy haze periods: implications for research,
844 Environmental Monitoring and Assessment, 186, 6097-6106, doi: 10.1007/s10661-014-3842-2,
845 2014.

846 Zhou, W., Mekic, M., Liu, J., Loisel, G., Jin, B., Vione, D., Gligorovski, S.: Ionic strength effects on the
847 photochemical degradation of acetosyringone in atmospheric deliquescent aerosol particles,
848 Atmospheric Environment, 198, 83-88, 2019.